RT Modelling for NDT Recent and Future Developments in the CIVA RT/CT Module

Roman FERNANDEZ [1], Laura CLEMENT [1], David TISSEUR [2], Ronan GUILLAMET [2], Marius COSTIN [2], Caroline VIENNE [2], Veronique COLOMBIE [2]
[1] EXTENDE, Massy, France
[2] CEA Saclay DIGITEO Labs, Gif-sur-Yvette, France

Contact e-mail: roman.fernandez@extende.com

Abstract. The CIVA platform dedicated to NDT modelling is widely used in different industrial sectors. X-ray/gamma ray radiography and tomography are commonly used as non-destructive evaluation method. Since 2011, the CIVA platform offers in addition to the radiography (RT) module a computed tomography (CT) module. This paper introduces the latest functionalities now available in CIVA RT/CT as well as current developments to be included in the future versions. In particular, high energy source types will be presented as well as modelling of new detectors and detectability criterion for the RT module. For the CT module, the development of reconstruction on helical scanning and non-standard trajectories and on-going work on scatter correction will be presented. Some examples will illustrate the applications of these developments.

1. Introduction

CIVA is the expertise platform which includes modelling plus imaging and analysis tools, assisting in the design and optimization of inspection methods and the prediction of their performances for realistic configurations. CIVA simulates Ultrasonic Testing (UT), Guided Wave Testing (GWT), Eddy Current Testing (ET), Radiographic Testing (RT) and Computed Tomography (CT).

The X-ray and Gamma ray simulation software CIVA (CIVA RT) has been developed to help the design stage of radiographic systems, to enable performance demonstration and to optimize the testing process [1]. The code takes the most influential parameters into account and allows simulation of a realistic and complex inspection configuration (source, specimen, defects, and detector) with a large usability to evaluate the defect detection, to elaborate mock-ups dedicated to Non Destructive Testing (NDT), and to perform detectors evaluation. The X-ray module models the full physics of photon-matter interaction in the range of 0.01 to 10 MeV, including photon scattering.

To increase the capabilities of CIVA, a computed tomography module based on the RT module was integrated in 2011 [2]. The CIVA CT module is able to simulate various tomographic configurations and perform the reconstruction with dedicated algorithms available to optimize the CT system by simulating photon interactions, to compare algorithms in the same framework, to estimate the influence of signal to noise ratio (SNR) in projections or the number of projections. This paper introduces the latest functionalities

now available in CIVA RT/CT as well as the current developments to be included in the future versions.

2. Methods

2.1. RT modelling

In order to model a realistic inspection, either in the Radiography Testing simulation module or in the Computed Tomography module, CIVA combines an analytical model and a Monte-Carlo method. The analytical model is used to calculate the images created from the direct radiation, while the Monte-Carlo model simulates the scattering effect. A combination of both models is then performed to give a realistic image. It is therefore possible to model the full RT system, including the part (specified as simple parametric geometrical forms or as complex forms through CAD formats such as stl, step or igs), the flaw, the X-ray or Gamma ray source and the detector (film, digital detector (DR) or computed radiography detector (CR)). The resulting image includes the influence of the source (size, spectrum and filtering), the attenuation and scattering, the photonic noise and the detector response. Depending on the type of detector used, the image will be displayed in optical density values for films or grey levels for digital detectors. The model behind film simulation is a Gray model developed by EDF [3] where the incident dose is converted into an optical density value. In a general way, the detectors are modelled in two successive steps. First a computation of the energy deposited on each pixel of the sensitive layer is realized. Then, depending on the modelled detector, a conversion of this energy into the appropriate physical value is performed.

2.2 CT modelling

Based on the RT computation method, the CT module allows the user to model a tomography scanning and then, as a second step, to perform the 3D reconstruction using an appropriate algorithm.

Until the latest version of CIVA (CIVA 2016), only circular tomographic scanning was available. For circular trajectories the standard FDK (Feldkamp-Davis-Kress) algorithm [4] is implemented, as well as an iterative one: PixTV [5]. The FDK (Feldkamp-Davis-Kress) algorithm is a 3D Fourier-based reconstruction method, considered as the gold standard in CT when SNR and projection numbers are large enough. PixTV is an iterative reconstruction algorithm which minimizes the TV (Total Variation) norm. It uses the linear data model for the CT problem like the classical deterministic algorithms. The projections and the imaged objects are discretized, i.e. they are represented by vectors or matrices.

Moreover, the software allows the import of experimental radiographic data, which can further be reconstructed with one of the analytic or iterative algorithms available. It is therefore directly possible in CIVA to compare experimental reconstructed results with simulated ones and moreover optimize the minimum number of projections required to get an accurate 3D reconstruction. Indeed, by reducing the number of projections and selecting the best algorithm it will lead to an optimization of the acquisition and a better preparation of the inspection.

3. Recent developments

Based on the existing features, tools and algorithms already available in the last version of CIVA some important developments were achieved in order to continue the improvements of the software and increase the range of applications.

3.1 High energy sources

In addition to the already implemented X-ray tube model, which can be used between 30 and 450 kV (simulating the physical phenomena involved in bremsstrahlung and characteristic photon productions) and gamma sources (created from spontaneous disintegration of radioactive elements as Iridium, Cobalt or Selenium which emit discrete rays), CIVA can now also model high energy sources such as Linear accelerators or Betatrons. The new release of CIVA comes with a library of three linear accelerators of 4 MeV, 6 MeV and 9 MeV and four Betatrons of 2 MeV, 6, MeV, 7.5 MeV and 9 MeV. Most of the spectra available in CIVA were modelled thanks to the Penelope Monte-Carlo code [6] and integrated into CIVA. The figure below illustrates a 6 and a 9 MeV linear accelerator (LINAC). Whatever the source, CIVA also takes into account its anisotropy during the computation of the direct and scattering phenomenon. This anisotropy is considered through a modification of the probability of emission of a given photon in function of the emitted angle. Experimental validations have been achieved [7] for 6 and 9 MeV LINAC on a 75 mm thickness 304L steel component including several notches of different apertures (from 20 µm up to 150 µm) with different orientations.

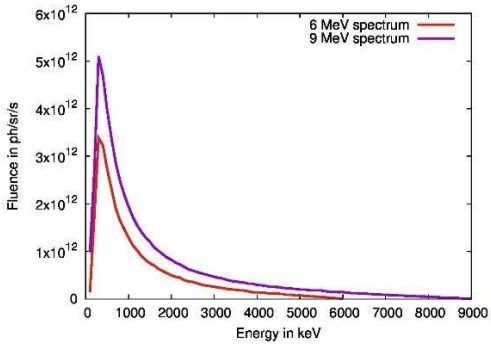

Fig. 1. 6-9 MeV spectra

3.2 Detectors

In addition to the already existing models available (2.1. RT modelling), a model was recently implemented in CIVA to better simulate experimental detectors. This detector called “generic detector” is modelled from experimental data contained in a calibration file and is based on the transfer function between measured incident dose and grey level. For each incident dose, mean grey level and standard deviation is computed in a region of interest. These measurements can be easily done with a step wedge where the Grey level will be extracted at the different material thicknesses. The figure below presents an example of a “generic detector” transfer function for ^{192}Ir.

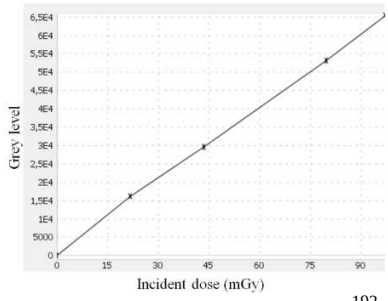

Fig. 2. Example of transfer function for ^{192}Ir source

3.3. Irradiated specimen

For nuclear applications, and in order to consider the potential presence of radioactive substances within solids that will have an impact on the darkening of the film a new functionality has been developed and integrated in the latest version of CIVA. This new model considers the influence of radioactive contamination on a cassette-film being in contact with an irradiating part. By activating the option "contact dose rate", the user can enter a "parasite" dose rate in contact of the film. This additional dose will be taken into account in the computation and in the final conversion of the dose to optical density on the radiogram. The example below compares a simulation of a pipe (50 mm thickness) made of steel with and without this additional dose. The source used in that example is a 120 Ci Iridium 192 gamma source and the film is a M100 type film. The first simulation is performed considering a clean part (with a contact dose rate equal to 0 mSv/h). In the second case, we considered a dose rate of 6.1 mSv/h. The time of exposure has been reduced in the second time in order to obtain the same incident dose on the detector as for the first case. Profile lines extracted on the optical density images are shown on Fig. 3.

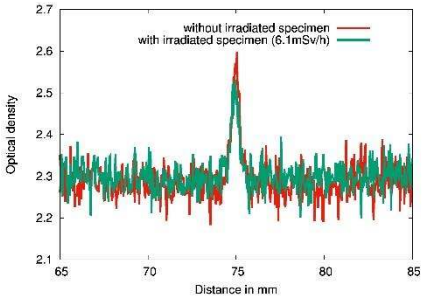

Fig. 3. Profile lines extracted on optical density images for a configuration without irradiated specimen and a second one with an irradiated specimen

It can be seen that for a same incident dose on the detector, the amplitude of the signal in the case where the irradiated specimen is modelled is inferior to the one obtained for the clean specimen. The irradiated specimen impacts the detectability of flaws.

3.4 Detectability criteria

One of the specifics of the RT technique is that the observation and statement of an indication is directly linked to the human eye. The interpretation can vary from one person to another one depending on this perception. Indeed, detection of an indication or accurate analysis of a film is faced with the problem of the performance of the human eye. In this context, two detectability criteria were implemented in the last version of CIVA (CIVA 2015) in order to help the user to determine whether the flaw simulated is seen or not for a given configuration. Both criteria are based on comparisons of contrast to noise ratio on the images with and without flaw.

3.4.1 Ellipse criterion:

This criterion has been developed for argentic film. The criterion defines the smallest surface interpretable by the eye (generally accepted as being a surface equal to 1.6mm²). From this surface an ellipse having the surface of 1.6mm² is defined that generates a square matrix named "convolution kernel" with an odd number of pixels along the edge. The values of the matrix are equal to 1 in the ellipse and 0 outside. Then, a computation of the "difference image" equal to the absolute value of the difference between the images with flaw and without flaw is performed in order to extract the visibility coefficient for each pixel of the image and the maximum of visibility of the image (where "imagdiff" is the "difference image" and "kernel" is the convolution kernel):

$$Visibility = Normalisation \times \sum_{i=0}^{i=nx} \sum_{j=0}^{j=ny} imagediff(i,j) \times kernel(i,j)$$

Eq 1. Formula for determining detectability by the human eye

The resulting detectability criterion is defined as the maximum of the visibility coefficients extracted in a total of 8 orientations of the ellipse in order to cover all the potential directions (angular step = 22.5°). Comparisons with experimental radiographic shots tend to show that the detection threshold is equal to 0.011.

3.4.2 *"Pseudo"* Rose criterion:

This criterion is based on the signal to noise ratio (SNR) for the detection of a uniform object balanced by the surface inspired by the Rose criterion [8]. The model implemented in CIVA is an alternative definition of the SNR where a ratio of mean grey value to standard deviation of the measured signal is extracted as detailed below where "surface" is the surface of the defect in pixels.

$$Rose\ criterion = \frac{Mean\ grey\ value\ in\ the\ flaw\ - Mean\ grey\ value\ in\ the\ flaw\ vicinity}{Max(variance\ in\ the\ flaw, variance\ in\ the\ flaw\ vicinity)} \times \sqrt{surface}$$

Eq 2. Formula for the « pseudo » Rose criterion in CIVA

The signal corresponds here to the contrast between the flaw and its background while the noise refers to the uncertainty of the measure. The Rose criterion states that a SNR of at least 5 is needed to be able to consider the indication as visible and is well adapted in the case of roughly circular flaws.

3.4.3 Fuchsia criterion:

It has been demonstrated that the Rose criterion shows its limits for cracks with an elongated shape or close to the limit of spatial resolution as well as for wire IQIs. In order to improve the performance of detectability criteria for conventional radiography (EN584 model), a new criterion has been developed and integrated in the latest version of CIVA. The Fuchsia criterion [9] inspired from the Rose one, is based on the knowledge that there is no direct equivalence between the visibility of step hole IQI and wire IQI. More particularly, by referring to French code "Design and Construction Rules for the Mechanical Components of PWR Nuclear Islands" (RCCM) [10], we can determine that a step hole IQI of diameter $\emptyset$ has a visibility equivalent to wire IQI of diameter $\emptyset/2.5$ (or $\emptyset/2.0$ for wire diameters > 1 mm). Furthermore, for conventional radiography, the noise modelled with EN584 model in CIVA depends on simulation pixel size. This leads to impact directly Rose criterion value. In practice, this pixel size does not account for a real

radiographic acquisition parameter and should not influence the noise level considered in the detectability criterion. To free ourselves from simulation parameters and model the human operator ability, we use a normalization method of the noise according to eye resolution. A large number of comparisons between simulations with this new criterion and experimental trials have been performed, providing very good results and showing that a detectability threshold of 1.5 can be considered. This new detectability criterion has been validated for films up to now.

3.5 Helical scan for Computed Tomography

Initially only the circular trajectory was modelled in CIVA for Computed Tomography simulations. The circular trajectory provides theoretically exact reconstructions only in the central plane of the object. However, when inspecting a long object, this acquisition geometry leads to severe artifacts in the reconstructed image. Helical or partially helical trajectories allow to handle this problem and theoretically exact algorithms were proposed [11]. Recently this scanning geometry was added and two reconstruction algorithms taken from literature were implemented with improvements with respect to the initial versions. The figure below illustrates the helical path in the CIVA 3D view of a multi-disk phantom.

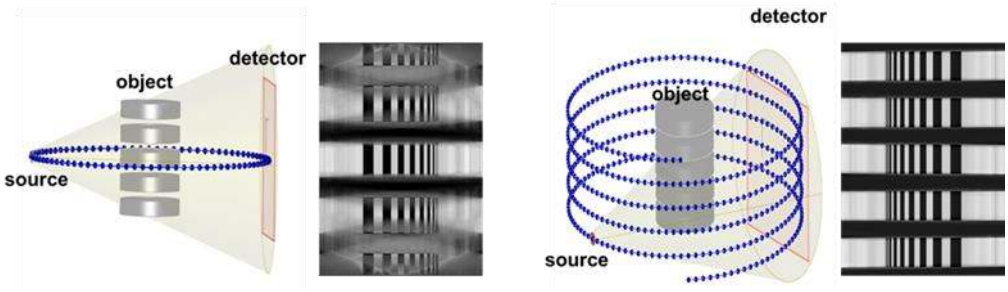

Fig. 4. CIVA CT scene and FDK reconstructions of the multi-disk phantom from circular (a) and helical (b) scanning geometries.

The multi-disk phantom illustrated in Fig. 4 is a test object that demonstrates the limits of the circular trajectory through severe artifacts towards the extremities of the object (Fig 4a). By contrast, the reconstruction on a helical scanning geometry is not affected by such artefacts (Fig 4b).

4. Current and on-going developments

After modelling in CIVA 2016 helical CT trajectories, advanced trajectories will be modelled in the future version of CIVA. First, short-scan trajectories, based on the helical one will be generated and adapted analytical reconstruction algorithms will be proposed (see Fig.5). Secondary, robotic trajectories will be modelled in the future versions of CIVA [12]. This trajectory will be generated from the reading of a text file with as many lines as path points, each line grouping the translations and rotations parameters of the source and detector relative to a reference.

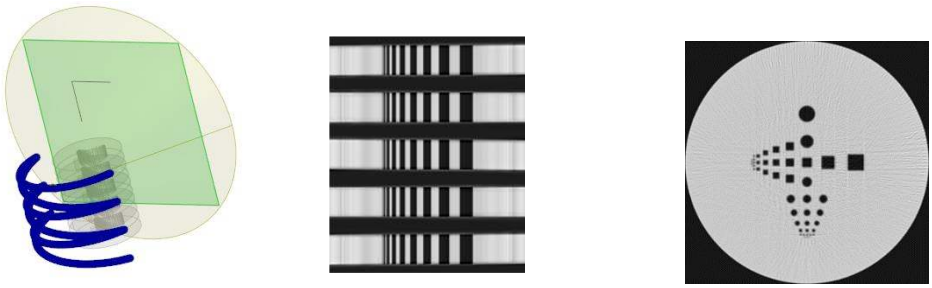

Fig. 5. Reconstruction of the multi-disk phantom using half-scan reverse helical trajectory

Iterative reconstruction algorithms based on standard iterative approach (SART and OSEM) will be developed to address such complex trajectories with nVidia CUDA implementation and adaptive RAM management used to reduce computation time and support 1024^3 voxels volumes.
CEA has developed a method for correction of scatter due to object and detector together using Scatter Kernel Superposition (SKS) [13] deconvolution method with a continuous approach. This method, illustrated in Fig.6, will be available next year.

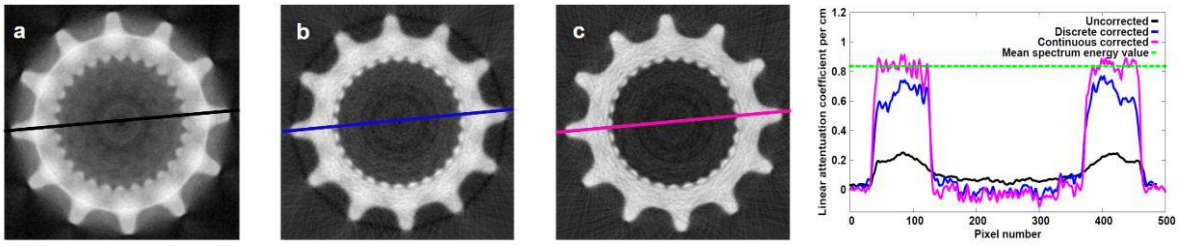

Fig. 6. Reconstruction slice of a) uncorrected projections b) corrected projections by discrete method c) corrected projections by continuous method and profiles comparison (right) [13].

Ring artifacts are CT phenomenon that occurs due to miscalibration of one or more elements in a CT scanner. In the future versions of CIVA, the user will have the possibility to correct these artefacts before the reconstruction of experimental data. Surface extraction of 3D data option will allow the user to save the surface rendering of a 3D CT reconstruction in a 3D cad file format that can be read in CIVA (*.STL). Developments are under progress to include in CIVA photon counting detectors type and X-ray phase imaging.

5. Conclusion

This paper illustrates some of the latest developments available in the CIVA RT-CT simulation platform. The capabilities of the modelling are continuously increasing to enlarge the scope of applications in the different domains requiring advanced NDT inspection and performance demonstrations. The RT modules allows now to easily model high energies sources taking into account a predefined linear accelerator or betatron and simulating the main photons matter interactions (such as pair creations that is an important physical phenomenon for such high energies). For nuclear applications, the users can account for irradiated specimen that may have a negative impact on the radiogram by generating a deterioration of the signal on a given indication. New detectors as well as an additional detectability criterion is also now available to enlarge the capabilities, make easier and more accurate the modelling and improve the analysis of results. Lastly, a new helical scanning trajectory has been integrated in the CIVA CT module to allow accurate reconstructions on long objects. The CIVA RT-CT module is in continuous development and new features are being added in order to meet the industrial needs.

6. References

[1] J.Tabary, P. Hugonnard, A.Schumm, R. Fernandez "Simulation studies of radiographic inspections with Civa", proceedings of the World Conference of NDT 2008
[2] R. Fernandez, M. Costin, D. Tisseur, A. Leveque, S.A. Legoupil, "CIVA Computed Tomography Modeling", proceedings of the World Conference of NDT 2012.
[3] A. Schumm, U. Zscherpel, "The EN584 standard for the classification of industrial radiography films and its use in radiographic modelling", in Proceedings of the Sixth International Conference on NDE in relation to structural integrity for nuclear and pressurized components, 2007.
[4] L.A. Feldkamp, I.C. Davis, J.W. Kress. "Practical cone-beam algorithm" . J. Opt. Soc. Am. A, 1(6):612–619, 1984.
[5] H. Wang, L. Desbat, S. Legoupil, "2D X-Ray Tomographic Reconstruction From Few Number of Projections And 3D Perspectives : Applications of Compressed Sensing Theory", 10th International Meeting on Fully Three-Dimensional Image Reconstruction in Radiology and Nuclear Medicine, Beijing, China, 2009.
[6] F. Salvat, J. M. Fernandez-Varea, J. Baro, J. Sempau, "PENELOPE, an algorithm and computer code for Monte Carlo simulation of electron-photon showers," Informes Tecnicos Ciemat, 799, CIEMAT, Madrid, Spain (1996)
[7] D. Tisseur, B. Rattoni, C. Vienne, R. Guillamet, G. Cattiaux, T. Sollier, "First Validation of CIVA RT Module with a Linear Accelerator in a Nuclear Context", proceedings of the World Conference of NDT 2016
[8] A. Rose, "The Sensitivity Performance of the Human Eye on an Absolute Scale", Journal of the optical society of America, Vol. 38, Number 2: 196-208, 1948
[9] D. Tisseur, C. Vienne, A.Schumm, P. Guérin, P. Duvauchelle, V. Kaftandjian, A. Peterzol Parmentier, U. Ewert , "A New Detectability Criterion for Conventional Radiography", proceedings of the World Conference of NDT 2016
[10] AFCEN, Design and Construction Rules for Mechanical Components of PWR Nuclear Islands RCC-M, Addendum : AFCEN, 1985.
[11] M. Costin, D. Tisseur, C. Vienne, R. Guillamet, H. Banjak, N. Bhatia, R. Fernandez, "CIVA CT, an advanced simulation platform for NDT", 6th Conference on Industrial Computed Tomography, Wels, Austria (iCT 2016)
[12] H. Banjak, M. Costin, C. Vienne, P. Duvauchelle, V. Kaftandjian, " X-ray Computed Tomography Reconstruction on Non-Standard Trajectories for Robotized Inspection", proceedings of the World Conference of NDT 2016
[13] N. Bhatia, D. Tisseur, F. Buyens et J. M. Létang, «Scattering correction using continuously thickness-Adapted Kernels,» NDT & E International, pp. 78:52-60, 2016.